Millimeter-Size Single-Crystal Graphene by Suppressing Evaporative Loss of Cu During Low Pressure Chemical Vapor Deposition

Shanshan Chen, Hengxing Ji, Harry Chou, Qiongyu Li, Hongyang Li, Ji Won Suk, Richard Piner, Lei Liao, Weiwei Cai, and Rodney S. Ruoff**

High-quality monolayer and multilayer graphene films have been synthesized on a variety of metal substrates by chemical vapor deposition (CVD),[1–4] and 30 inch monolayer films (along the diagonal) have been reported.[5] These CVD processes have typically yielded polycrystalline graphene films composed of relatively small graphene grains (also called domains).[6,7] The higher density of grain boundaries degrades the physical and chemical properties of the graphene such as strength,[8,9] electrical mobility,[10] thermal conductivity,[11] and oxidation resistance.[6] Thus, it is desirable to prepare large single-crystal graphene to minimize the impact of defects found at grain boundaries. Millimeter-size single crystal graphene has previously been achieved on noble metals such as Pt[12] or single crystal Ru(0001)[13] or Ni(111),[14] but a more cost-effective method is necessary for industrial-scale implementation. Recent reports from a few groups have reported sub-millimeter-size (~0.5 mm) single-crystal graphene deposited on polycrystalline Cu either by low-pressure CVD in a Cu enclosure,[15] or by ambient pressure CVD by suppressing nucleation through annealing.[16] Wu et al.[17] and Yan et al.[18] reported the growth of millimeter-sized graphene domains through ambient pressure CVD and controlled chamber pressure CVD (108 Torr), respectively. In our work, we show the synthesis of ~2 mm single crystal graphene via low pressure CVD, and the large size domains were achieved through the suppression loss of Cu by evaporation which is reported for the first time. The method and results presented here provide some insight into the nucleation mechanism and pave the way to large size graphene single crystals.

By suppressing loss of Cu (by evaporative loss) of the Cu substrate at the high temperature and low pressure growth conditions, single-crystal graphene domains up to ~2 mm across along the diagonal were obtained,[12,15,16] and with some crystals having a carrier mobility of over 5200 $cm^2 V^{-1} s^{-1}$.

As shown in **Figure 1**a, Cu tubes formed out of Cu foil were used as substrates for the CVD-grown graphene (two additional substrate configurations will be discussed later). The CVD growth was carried out in a one inch quartz tube furnace with a relatively lower methane flow rate[19] of 0.1 sccm (partial pressure of 9 mTorr) and a hydrogen flow rate of 10 sccm (partial pressure of 65 mTorr) at 1035 °C, following a 15 min hydrogen anneal (2 sccm, 22 mTorr). The as-received Cu foil (99.8% Alfa Aesar no. 13382) was electropolished to smooth the surface and to remove a coating layer applied by the manufacturer (see Experimental Section). The foil was then wrapped into a long tube (5 cm) with a diameter of 0.5 cm. During the high temperature anneal and growth, the copper atoms on the outer surface of the Cu tube were evaporated and removed by the vacuum, while the copper atoms on the inner surface evaporated but re-deposited so that the evaporative loss of Cu from the inner surface was strongly suppressed. Indeed, the inside volume of the Cu tube likely has established equilibrium between Cu vapor and Cu foil. A representative schematic is depicted in Figure 1b.

After 6 h of exposure to methane and hydrogen, the sample was cooled to room temperature and removed; the topography of both the inner surface (no loss of Cu) and outer surface (loss of Cu by evaporation) of the Cu tube were measured using contact-mode atomic force microscopy (AFM) (Veeco, Autoprobe CP Research System). **Figures 2**a and Figures 2b are AFM images of the inner and outer surfaces of the Cu tube. Both surfaces show similar terrace-like morphologies[1] which indicates that both were covered and passivated by graphene.[6] However, the outer surface of the tube is very rough, with trenches several hundred nanometers in depth. This roughness is evidence that this surface experienced considerable loss of Cu by evaporation during graphene growth. In contrast, the inner surface roughness is about a tenth that of the Cu tube exterior, as can be seen in the line scans in Figure 2c. It has been stated that graphene nucleation is enhanced on rough regions[20,21] or rippled structures,[22] and polished Cu foils have been shown to yield larger graphene domains.[20,23] On the outer surface of the Cu tube, we found that graphene domains preferentially nucleate on the rough surface as studied by AFM (see Figure S1

Prof. S. Chen, Q. Li, H. Li, Prof. W. Cai
Department of Physics
Laboratory of Nanoscale Condense Matter Physics and State Key Laboratory of Physical Chemistry of Solid Surfaces
Xiamen University
Xiamen, 361005, China
E-mail: wwcai@xmu.edu.cn
Prof. S. Chen, Dr. H. Ji, H. Chou, Dr. J. W. Suk, Dr. R. D. Piner, Prof. R. S. Ruoff
Department of Mechanical Engineering and the Materials Science and Engineering Program
The University of Texas at Austin
Austin, TX 78712, USA
E-mail: r.ruoff@mail.utexas.edu
Prof. L. Liao
Department of Physics
Wuhan University
Wuhan, 430072, China.

DOI: 10.1002/adma.201204000

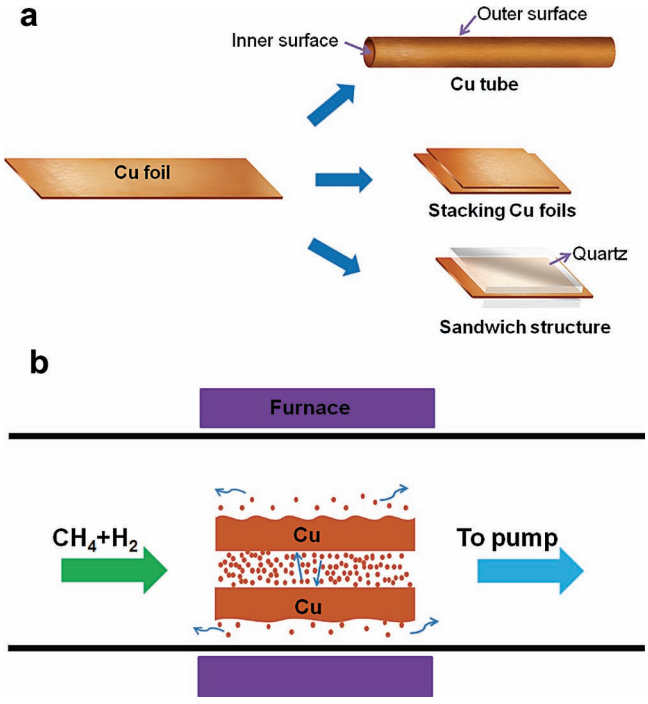

Figure 1. a) Cu tube, stacked Cu foils, and Cu foil between two quartz slides, prior to graphene growth. b) Illustration depicting the suppression of loss of Cu by evaporation and redeposition in a confined space during low pressure CVD growth of graphene.

in the Supporting Informations). However, during the growth the evaporation of Cu could also induce roughness especially when performing long time growth aiming for larger domains. Through the long Cu tube, the loss of Cu by evaporation

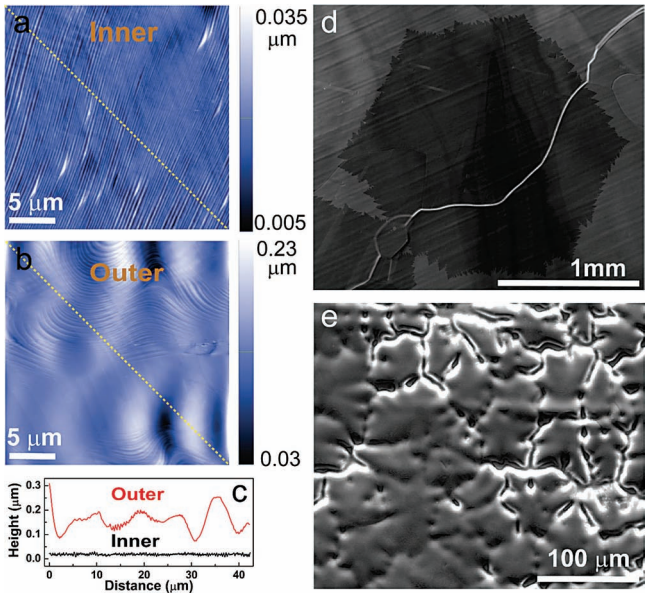

Figure 2. a,b) AFM images of graphene grown on the inner (a) and outer (b) surfaces of the Cu foil tube. c) Line profiles of positions indicated in (a) and (b). d,e) SEM images of graphene on the inner (d) and outer (e) surfaces of the Cu foil tube.

in the middle of the tube is suppressed (since any Cu that evaporates is re-deposited, and the cylindrical symmetry favors essentially equal evaporation and re-deposition at all regions on the interior surface) and this evidently results in a smoother Cu surface during long, high temperature processes. Thus, the smooth inner surface facilitated a much lower nucleation density and much larger graphene domains. It is also possible that the flux of Cu atoms in the gas phase, either through collisions with methane molecules in the gas phase or collisions with the Cu surface, is playing a role. For example it is not inconceivable that evaporated Cu atoms bury small nuclei and that other nuclei grow the larger islands. At 1035 °C the vapor pressure of Cu in equilibrium is 1.42×10^{-4} Torr[24] and it is estimated that prior to significant coverage of the inner surface by graphene (which inhibits evaporation of Cu beneath it) roughly 10 layers are depositing on all of the inner surface every second, with an assumed sticking coefficient of 1. We can therefore see that one might speculate about possible contributions of the evaporated Cu atoms, along with the role of the smoother surface.

Millimeter-size graphene single-crystals were found on this smooth inner surface of the Cu tube. Figure 2d shows a large graphene domain. Note that this large graphene domain spans two adjacent Cu grains. Despite maintaining growth conditions over long times (6 h), we did not achieve full surface coverage. After 6 h, large single-crystal graphene domains up to ~2 mm along the diagonal direction were obtained, and we observed that the domains often crossed Cu grain boundaries. In contrast to the inner surface, the nucleation density on the outer surface was more than two orders higher, which allowed for nearly full coverage (Figure 2e). In addition, by applying a two-step growth process,[19] a complete film could be obtained on both the inner and outer surfaces by increasing the methane flow rate to 7 sccm and partial pressure to 1 Torr for 3 min, after the 6 h growth.

In this experimental setup, growth conditions including the temperature and the partial pressure of methane and hydrogen are the same inside and outside of the Cu tube. It seems that the main difference between the inner and outer surfaces is the surface roughness. In order to isolate the role of surface roughness, a control growth was done on a tube formed with Cu foil which had been pre-annealed (15 min, 1035 °C) before loading into the CVD chamber. This control sample was found to have evaporation-assisted roughness on both foil surfaces (see Figure S2 in the Supporting Information). This control Cu tube was inserted with a non-annealed Cu foil tube (see the Supporting Information). The pre-annealed Cu foil tube had a much higher graphene nucleation density compared to the non-annealed Cu foil tube (see Figure S3 in the Supporting Information).

In order to further test this method, other configurations were devised. Two different structures were prepared for synthesis; in one case, two separate Cu foils were stacked together so that they were physically contacting, and in another, a sandwich structure with two Cu foils clipped in between two opposing quartz slides with a gap between them was used (Figure 1a). Under the same growth conditions as mentioned above, a ~1.9 mm graphene domain was achieved on the inner surface of the *stacked foil*, and an adlayer in the middle of the domain was observed. The *sandwich structure* yielded graphene domains

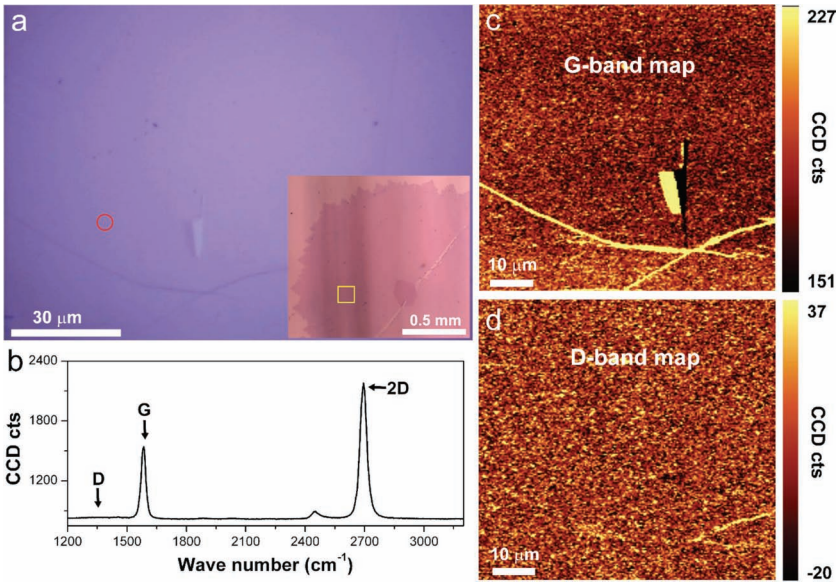

Figure 3. a) Optical micrograph of the square region from the millimeter-size graphene domain (see Inset) transferred onto a 300 nm SiO_2/Si substrate. b) Raman G-band mapping of the graphene domains taken from (a). c) Raman spectra of the graphene taken from the red circle position in (a).

that were separated by several millimeters after 3h growth (see Figure S4 in the Supporting Information). This sparse nucleation and large domains validates the influence of the enclosed environment and perhaps the roles of a smoother surface and/or of the dynamic environment present (a relatively high rate of evaporation and redeposition of Cu on the inside surfaces, a relatively high vapor pressure of Cu atoms in the gas phase in, or close to in, equilibrium with the Cu(s)).

Figure 3a shows an optical micrograph of a portion of the millimeter-size graphene domain transferred onto a 300 nm SiO_2/Si substrate. An area with a small crack was selected to show the uniform optical contrast of the graphene sheet, which indicates its uniform thickness. Raman spectroscopy was used to characterize the quality, thickness, and uniformity of the as-grown graphene domains. Figures 3c and Figure 3d show a Raman map of the G-band (1580 cm^{-1}) and D-band (1350 cm^{-1}), respectively, taken from the area in the orange rectangle shown in Figure 3a. A typical Raman spectrum is shown in Figure 3c, which exhibits sharp G and 2D peaks with a small G/2D peak ratio of ~0.3. This spectrum shows that the film is a single layer graphene sheet. Furthermore, the disorder-induced D band is not detected on the graphene sheet, as the intensity map shown in Figure 3d is uniform and indistinguishable from the graphene and crack region, which indicates a high quality film.

The structure of the millimeter-sized domains was determined by transmission electron microscopy (TEM) (JEM-2010F). A low magnification SEM image of the millimeter-size domains after they were transferred onto a Quantifoil holey carbon supported grid is shown in **Figure 4**a. Two adjacent domains (**D1** and **D2**) covered half of the grid. We performed a complete survey of each domain assessed by TEM, by obtaining selected area electron diffraction (SAED) data from every square in the grid that was coated by each graphene domain. This exhaustive SAED survey showed the domains were single crystal. Typical examples of the SAED data on domain **D1** are shown in Figure S5 in the Supporting Information. For example, SAED were tested on 9 different sites on each square as shown in Figure 4b. Special attention was given on to the edge region (red dotted circle in Figure 4c) where the lobes are and the regions where the lobes join together (green dotted circle in Figure 4c). The results shown in Figures 4e and Figure 4f indicate that each domain has only one a single, uniform SAED pattern that matches that expected for monolayer graphene. The boundary between two graphene grains is marked with a blue dashed line. A careful survey on the boundary region of the two adjacent domains depicts the lobe morphology where two domains are joined together. A 25° rotation angle between **D1** and **D2** was observed on the boundary of the two domains as shown in Figure 4g. SAED surveys of 23 randomly chosen graphene domains confirmed that each was a single crystal and that the inter-domain mis-orientation angles are random.

The electrical transport properties were measured by a Lakeshore probe station with an Agilent 4155 C in ambient condition at room temperature. For the electrical characterization, the graphene sheets were first transferred onto a highly doped p-type silicon substrate with a 300 nm thick thermal silicon oxide layer, and then contacted by e-beam lithography and a metallization process to define the external and drain electrodes.[25,26] A typical channel width and length were 4.2 and 18.1 μm, respectively (see Supporting Information). The

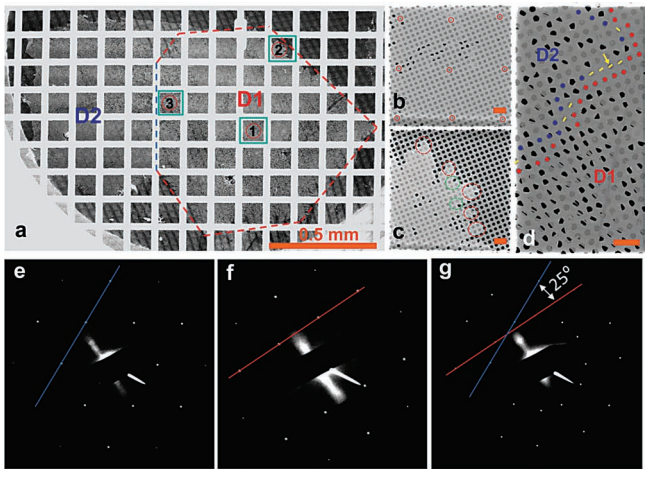

Figure 4. a–d) SEM images of graphene transferred onto a Quantifoil TEM grid. Higher magnification of corresponding squares in 1 (b), 2 (c) and 3 (d). The scale bars in (b–d) are 10 μm. e–g) TEM SAED of graphene taken from the graphene domain D2 (e), D1 (f) and region marked with a yellow arrow in (d).

source-drain conductance was measured at room temperature as a function of back-gate voltage. The mobility for these millimeter-size single crystal graphene films was found to be up to 5200 $cm^2 V^{-1} s^{-1}$ (see Figure S6 in the Supporting Information), which is relatively higher than the values obtained from our previous work,[1,15] typical values were in the range of 2000 to 5200 $cm^2 V^{-1} s^{-1}$.

In conclusion, millimeter-size single-crystal monolayer graphene was synthesized on the inner surface of Cu foil in several different configurations (stacked and physically contacting, stacked but separated, rolled into a cylinder) in a tube furnace. When the Cu in the inner surface evaporates it redeposits on the inner surface, and so no or little Cu is lost (a small amount of loss of Cu might occur at the open ends) and we found this surface to be much smoother than the outer surface in identical CVD growth conditions. SEM, Raman spectroscopy, TEM with SAED, and FET measurements showed that the graphene domains had a single crystallographic orientation with carrier mobility as high as 5200 $cm^2 V^{-1} s^{-1}$.

Experimental Section

Electropolishing of Cu Foil: The copper foil was electropolished using a home-built electrochemical cell. The 25 μm thick Cu foil (99.8%, Alfa-Aesar, item no. 13382) was used as an anode with a large Cu plate as the cathode; the electropolishing solution was composed of 300 mL of water, 150 mL of ortho-phosphoric acid, 150 mL of ethanol, 30 mL of isopropyl alcohol, and 3 g of urea. The Cu foil was placed into the solution while it was supported by an alligator clip. A Hewlett-Packard 6612 System DC power supply was used to supply constant voltage/current, and a voltage in the range of 3.0–6.0 V was applied for 90 s. After electropolishing, the Cu foil was rinsed with deionized water, then further washed with ethanol, and finally blow-dried with nitrogen.

Supporting Information

Supporting Information is available from the Wiley Online Library or from the author.

Acknowledgements

We appreciate comments by C. Ventrice, Jr. The work at UT Austin was supported by the National Science Foundation Grant #1006350 and the Office of Naval Research. The work at Xiamen University was supported from the National Natural Science Foundation of China through grant nos. 91123009 and 10975115, and the Natural Science Foundation of Fujian Province of China (No. 2012J06002).

Received: September 24, 2012
Revised: December 2, 2012
Published online: February 6, 2013

[1] X. S. Li, W. W. Cai, J. H. An, S. Kim, J. Nah, D. X. Yang, R. Piner, A. Velamakanni, I. Jung, E. Tutuc, S. K. Banerjee, L. Colombo, R. S. Ruoff, *Science* **2009**, *324*, 1312.
[2] K. S. Kim, Y. Zhao, H. Jang, S. Y. Lee, J. M. Kim, J. H. Ahn, P. Kim, J. Y. Choi, B. H. Hong, *Nature* **2009**, *457*, 706.
[3] A. Reina, X. T. Jia, J. Ho, D. Nezich, H. B. Son, V. Bulovic, M. S. Dresselhaus, J. Kong, *Nano Lett.* **2009**, *9*, 30.
[4] S. S. Chen, W. W. Cai, R. R. Piner, X. S. Li, J. W. Suk, Y. P. Wu, Y. J. Ren, J. Y. Kang, R. S. Ruoff, *Nano Lett.* **2011**, *11*, 3519.
[5] S. Bae, H. Kim, Y. Lee, X. F. Xu, J. S. Park, Y. Zheng, J. Balakrishnan, T. Lei, H. R. Kim, Y. I. Song, Y. J. Kim, K. S. Kim, B. Ozyilmaz, J. H. Ahn, B. H. Hong, S. Iijima, *Nat. Nanotechnol.* **2010**, *5*, 574.
[6] S. S. Chen, L. Brown, M. Levendorf, W. W. Cai, S. Y. Ju, J. Edgeworth, X. S. Li, W. C. Magnuson, A. Velamakanni, R. R. Piner, J. Y. Kang, J. Park, R. S. Ruoff, *ACS Nano* **2011**, *5*, 1321.
[7] J. M. Wofford, S. Nie, F. K. McCarty, N. C. Bartelt, O. D. Dubon, *Nano Lett.* **2010**, *10*, 4890.
[8] R. Grantab, B. V. Shenoy, R. S. Ruoff, *Science* **2010**, *330*, 946.
[9] M. A. Haque, M. T. A. Saif, *Proc. Natl. Acad. Sci. USA* **2004**, *101*, 6335.
[10] Q. F. Lei, R. S. Lin, D. Y. Ni, Y. C. Hou, *J. Chem. Eng. Data* **1997**, *42*, 971.
[11] A. Bagri, S. P. Kim, R. S. Ruoff, B. V. Shenoy, *Nano Lett.* **2011**, *11*, 3917.
[12] L. B. Gao, W. C. Ren, L. H. Xu, L. Jin, Z. X. Wang, T. Ma, L. P. Ma, Z. Y. Zhang, Q. Fu, M. L. Peng, H. X. Bao, M. H. Cheng, *Nat. Commun.* **2012**, *3*, 699.
[13] Y. Pan, H. G. Zhang, D. X. Shi, J. T. Sun, S. X. Du, F. Liu, H. J. Gao, *Adv. Mater.* **2008**, *20*, 1.
[14] T. Iwasaki, H. J. Park, M. Konuma, D. S. Lee, H. J. Smet, U. Starke, *Nano Lett.* **2011**, *11*, 79.
[15] X. S. Li, W. C. Magnuson, A. Venugopal, M. R. Tromp, J. B. Hannon, M. E. Vogel, L. Colombo, R. S. Ruoff, *J. Am. Chem. Soc.* **2011**, *133*, 2816.
[16] H. Wang, G. Wang, P. Bao, S. Yang, W. Zhu, X. Xie, W.-J. Zhang, *J. Am. Chem. Soc.* **2012**, *134*, 3627.
[17] T. Wu, G. Ding, H. L. Shen, H. M. Wang, L. Sun, D. Jiang, X. M. Xie, M. h. Jiang, *Adv. Funct. Mater.* **2012**, DOI: 10.1002/adfm.201201577.
[18] Z. Yan, J. Lin, Z. W. Peng, Z. Z. Sun, Y. Zhu, L. Li, S. C. Xiang, E. L. Samuel, C. Kittrell, M. J. Tour, *ACS Nano* **2012**, *6*, 9110.
[19] X. S. Li, C. Magnuson, A. Venugopal, J. H. An, J. W. Suk, B. Han, M. Borysiak, W. W. Cai,, R. S. Ruoff, *Nano Lett.* **2010**, *10*, 4328.
[20] Z. T. Luo, Y. Lu, W. D. Singer, E. M. Berck, L. A. Somers, B. R. Goldsmith, A. T. C. Johnson, *Chem. Mater.* **2011**, *23*, 1441.
[21] H. Kim, C. Mattevi, R. M. Calvo, J. C. Oberg, L. Artiglia, S. Agnoli, C. F. Hirjibehedin, M. Chhowalla, E. Saiz, *ACS Nano* **2012**, *6*, 3614.
[22] T. M. Paronyan, M. E. Pigos, G. G. Chen, R. A. Harutyunyan, *ACS Nano* **2011**, *5*, 9619.
[23] G. H. Han, F. Gunes, J. J. Bae, E. S. Kim, S. J. Chae, H. J. Shin, J. Y. Choi, D. Pribat, Y. H. Lee, *Nano Lett.* **2011**, *11*, 4144.
[24] R. E. Honig, D. A. Kramer, *RCA Rev.* **1969**, *30*, 285.
[25] L. Liao, J. Bai, Y. Qu, Y.-C. Lin, Y. Li, Y. Huang, X. Duan, *Proc. Natl. Acad. Sci. USA* **2010**, *107*, 6711.
[26] R. Martel, T. Schmidt, R. H. Shea, T. Hertel, P. Avouris, *Appl. Phys. Lett.* **1998**, *73*, 2447.